



# Lipid-coated hydrogel shapes as components of electrical circuits and mechanical devices

K. Tanuj Sapra & Hagan Bayley

Department of Chemistry, University of Oxford, Oxford OX1 3TA, UK.

SUBJECT AREAS:  
MATERIALS SCIENCE  
MATERIALS CHEMISTRY  
SYNTHETIC BIOLOGY  
BIOPHYSICS

Received  
4 April 2012

Accepted  
30 October 2012

Published  
14 November 2012

Correspondence and requests for materials should be addressed to K.T.S. (tanuj.sapra@chem.ox.ac.uk)

Recently, two-dimensional networks of aqueous droplets separated by lipid bilayers, with engineered protein pores as functional elements, were used to construct millimeter-sized devices such as a light sensor, a battery, and half- and full-wave rectifiers. Here, for the first time, we show that hydrogel shapes, coated with lipid monolayers, can be used as building blocks for such networks, yielding scalable electrical circuits and mechanical devices. Examples include a mechanical switch, a rotor driven by a magnetic field and painted circuits, analogous to printed circuit boards, made with centimeter-length agarose wires. Bottom-up fabrication with lipid-coated hydrogel shapes is therefore a useful step towards the synthetic biology of functional devices including minimal tissues.

Issues and organs are organized cellular assemblages capable of internal and external communication by means of chemical, electrical and mechanical signals<sup>1,2</sup>. An important undertaking of synthetic biologists is the realization of minimal cells (protocells)<sup>3</sup> and minimal tissues (prototissues)<sup>4</sup>. Like their natural counterparts, synthetic minimal tissues should be compartmented, and able to communicate and support emergent properties. Communication might be through chemical (e.g., the movement of ions or small molecules) or physical (e.g., the detection of force or electrical potentials) means.

Up to now, lipid vesicles have been the system of choice for the development of artificial cells<sup>5–7</sup>. However, the small size of these compartments limits their manipulation, including the ability to measure ionic currents through the bilayer envelopes. Systems based on droplet interface bilayers (DIB) can be more readily controlled<sup>8</sup>. A DIB is formed when two lipid monolayer-coated aqueous droplets in an oil are brought together. Several such droplets can be assembled to form a network, and when membrane proteins are included in the DIBs, functional systems are produced<sup>8</sup>. DIBs including those formed on hydrogels have been used to study the fundamental properties of membrane proteins<sup>9–14</sup>, and aqueous DIB networks have been used to construct devices<sup>12</sup>, including a light sensor<sup>8</sup>, a battery<sup>8</sup>, and half- and full-wave rectifiers<sup>15</sup>. Recently, droplet networks that function in aqueous media have been devised<sup>16</sup>. In a synthetic biology context, these networks can be regarded as minimal tissues<sup>4</sup>.

However, aqueous droplet networks are delicate. Robust 3D systems that incorporate engineered membrane proteins for inter-compartment communication are required. Hydrogels are ideal scaffolds to realize such systems; they conduct ions, they can be molded, and many are biocompatible. Here, we present a simple approach in which shaped lipid-coated hydrogel objects are used to assemble networks both with and without bilayers between them. Both proved useful in devices. The hydrogel bilayer networks employ electrical and chemical signals for communication, and are capable of performing electrical and mechanical tasks. The modular hydrogel system expands the scope of DIB networks by enabling the construction of devices with enhanced structural complexity and functionality (Fig. 1), which has not been achieved thus far with aqueous droplets.

## Results

Lipid monolayers self-assemble on various shaped objects made from a hydrogel and immersed in a lipid/oil mixture (Fig. 1a). As described in detail below, depending on the lipid concentration in the oil and the force applied to the objects, we have been able to (i) form bilayers between two millimeter-sized hydrogel shapes (with 1–5 mg mL<sup>-1</sup> 1,2-diphytanoyl-*sn*-glycero-3-phosphocholine (DPhPC) in hexadecane) by controlling the distance between the objects with a micromanipulator (Fig. 1b); (ii) form stable patterned assemblies with bilayers between more than two hydrogel shapes without the need for precision control with a micromanipulator (10 mg

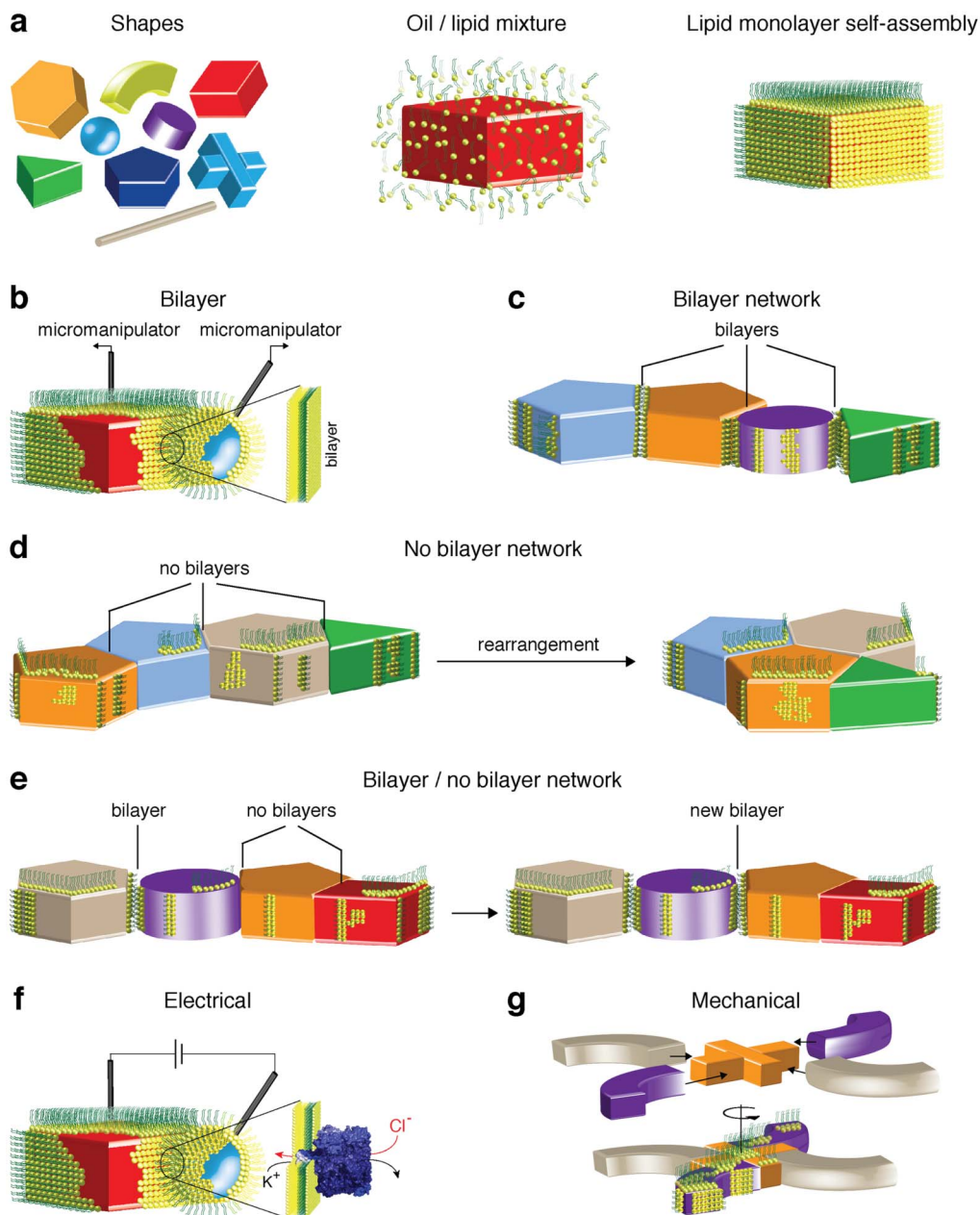


**Figure 1 | Lipid-coated hydrogel networks.** (a) Hydrogel objects with various shapes immersed in a lipid/oil solution become coated with a lipid monolayer. (b) When two lipid-coated shapes are brought together with a micromanipulator, a bilayer can be formed at the interface. (c) At high lipid concentrations, a stable bilayer network is formed. (d) When the shapes are pressed against each other, the bilayers rupture at the hydrogel interfaces, and a network coated with a single external lipid monolayer is obtained. The positions of the hydrogel shapes in both bilayer and no-bilayer networks can be rearranged to change the network topology. (e) Networks can be formed with and without bilayers between specific hydrogel objects. In such a network, a new bilayer can be created between two shapes (which did not originally have a bilayer) by pulling them apart and forming the bilayer by bringing them back together. Bilayer networks can be used to form functional electrical and mechanical devices. (f) For example,  $\alpha$ HL pores can be used to carry an ionic current between two hydrogel shapes separated by an interface bilayer. (g) A hydrogel rotor is an example of a mechanical device.

$\text{mL}^{-1}$  DPhC) (Fig. 1c); (iii) self-assemble hydrogel shapes in arbitrary patterns without bilayers between the shapes (up to  $5 \text{ mg mL}^{-1}$  DPhC) and later rearrange the assemblies in patterns of specific design (Fig. 1d); and (iv) build hydrogel networks with a bilayer between some shapes and none between the others ( $5\text{--}10 \text{ mg mL}^{-1}$  DPhC) (Fig. 1e). A high lipid concentration ( $>5 \text{ mg mL}^{-1}$  DPhC) is required to stabilize a bilayer network. However, even at high lipid concentrations, bilayers between hydrogel objects can be ruptured and expelled by applying a force to the objects that results in pressure normal to the bilayer surface.

**Bilayer formation between hydrogel shapes.** A lipid monolayer is formed on a hydrogel surface upon immersion in a lipid / oil mixture. Previously, an individual bilayer has been formed at the interface of an aqueous droplet and a flat hydrogel surface<sup>11,14,17</sup>. We supposed that two hydrogel shapes, encased in lipid monolayers, brought close to each other with a micromanipulator, would form a bilayer at the interface (Fig. 1b), which could be functionalized by the incorporation of transmembrane pores (Fig. 1f). To test this, initially, hydrogel spheres were brought into contact with other hydrogel shapes (Fig. 2a–d, Supplementary Fig. S1). When two

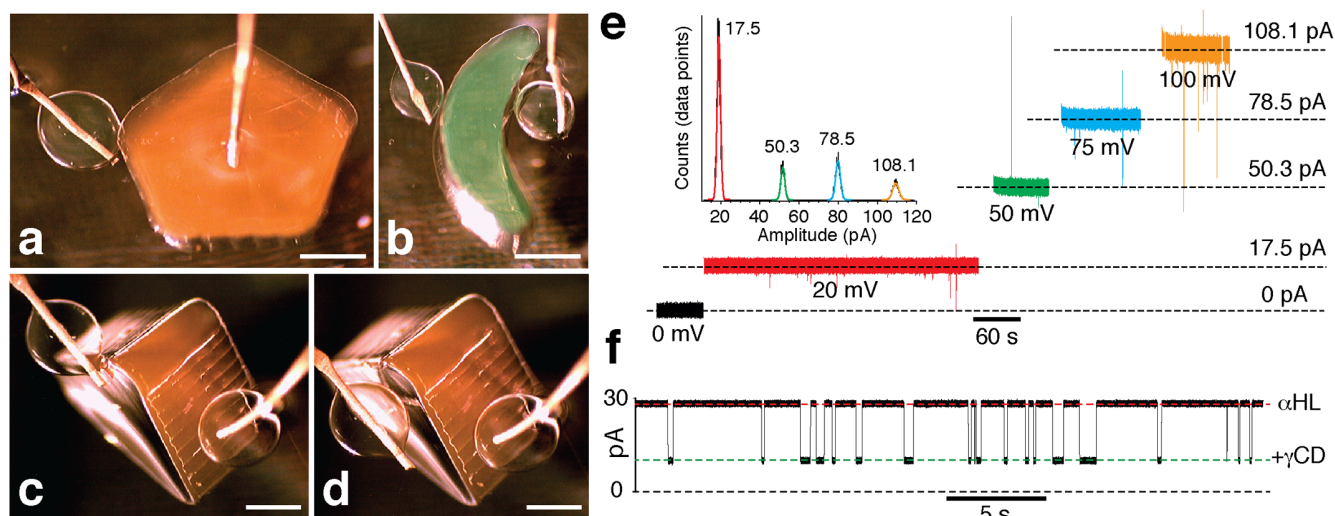


**Figure 2 | Hydrogel-hydrogel interface bilayers.** Various agarose shapes (1% w/v) were made with a PMMA mold (Supplementary Fig. S1). A lipid monolayer self-assembled on the hydrogel shapes when they were immersed in a lipid/hexadecane solution ( $5 \text{ mg mL}^{-1}$  DPhPC). (a, b) The existence of an interface bilayer between two hydrogels was demonstrated by using a lipid-coated agarose sphere and a different shape. When the two objects were brought together, bilayer formation was observed by an increase in capacitance. To prove that a hydrogel shape was completely covered with a lipid monolayer, a lipid-coated agarose sphere ( $\sim 1 \text{ mm}$ ) was used to touch the shape at arbitrary positions (c, d). Bilayer formation was observed each time. Scale bars (a–d), 1 mm. (e) A hydrogel-hydrogel interface bilayer permitted the insertion of  $\alpha$ HL pores. Heptameric WT- $\alpha$ HL ( $\sim 0.2 \mu\text{L}$ ,  $1.1 \mu\text{g mL}^{-1}$ ) diluted in DPhPC liposomes ( $1 \text{ mg mL}^{-1}$ ) in 1 M KCl, 10 mM Tris.HCl, pH 7.0, was absorbed on an agarose sphere connected to the ground electrode (denoted *cis*). The sphere was then brought in contact with another agarose sphere connected to the active electrode (denoted *trans*) to form a bilayer and insertion of  $\alpha$ HL was monitored (Supplementary Fig. S8). The currents carried by a single  $\alpha$ HL pore upon increasing the potential applied to the *trans* electrode (+20, +50, +75 and +100 mV) were 17.5 pA, 50.3 pA, 78.5 pA and 108 pA, respectively, in agreement with reported values<sup>42</sup>. (f) The inclusion of  $\gamma$ CD ( $50 \mu\text{M}$ ) in one of the agarose spheres (*trans*) elicited binding events with the  $\alpha$ HL mutant 2N (*cis*) with  $\sim 64\%$  block of the amplitude of the open pore current ( $n = 562$  events, from two independent experiments). The residence time of  $\gamma$ CD was  $146 \pm 4 \text{ ms}$  at +20 mV. The signal was low-pass filtered at 1 kHz and sampled at 10 kHz.

lipid-coated hydrogel surfaces were brought together, a bilayer indeed formed between them, which was detected by an increase in specific capacitance to the anticipated value (Supplementary Fig. S2). Assuming a circular bilayer, the specific capacitance of the bilayers formed between two hydrogels was determined to be  $0.56 \pm 0.14 \mu\text{F cm}^{-2}$  (average  $\pm$  S.D.,  $n = 11$ ). This value is in good agreement with the reported value of  $\sim 0.65 \mu\text{F cm}^{-2}$ <sup>18</sup>.

These hydrogel-hydrogel interface bilayers were stable ( $\geq 2 \text{ h}$ ) under an applied potential (+50 mV to +150 mV) (Supplementary Fig. S2). An electrical connection between two hydrogel shapes could be established through staphylococcal  $\alpha$ -hemolysin ( $\alpha$ HL) pores inserted in the lipid bilayer (Fig. 2e; Supplementary Fig. S8a,b). The integrity of the  $\alpha$ HL pores was confirmed by using the E111N/K147N (2N) mutant of  $\alpha$ HL and observing  $\gamma$ -cyclodextrin ( $\gamma$ CD) binding (Fig. 2f). The residence time of  $\gamma$ CD within the pore at +20 mV was  $146 \pm 4 \text{ ms}$  (average  $\pm$  S.D.,  $n = 562$ ).

With a sphere against a flat hydrogel shape, we measured bilayer capacitance values of up to 800 pF. Based on a specific capacitance of  $0.65 \mu\text{F cm}^{-2}$ <sup>18</sup>, this value indicates a bilayer surface area of  $\sim 0.1 \text{ mm}^2$ . Attempts to increase the bilayer area by pushing the sphere against the flat hydrogel surface by using a micromanipulator resulted in rupture of the bilayer. Stable millimeter-sized bilayers (up to  $\sim 2.5 \text{ mm}^2$ ) could be formed ( $1\text{--}5 \text{ mg mL}^{-1}$  DPhPC in hexadecane) by carefully bringing the flat faces of two hydrogel objects, such as hexagons, pentagons, cubes, cylinders and crosses, close to each other with a micromanipulator (Fig. 3; Supplementary Fig. S2). A bilayer thus formed was  $\sim 20$ -times larger in area than a bilayer formed between a sphere and a flat surface. Bilayers could also be formed between surfaces with alternative curvatures. For example, two crescent-shaped hydrogels formed bilayers between their convex surfaces (Fig. 3b), and between the two horns of the crescents (Fig. 3c). Complementary regions of two objects could be fit in a

lock-and-key arrangement with a bilayer at the interface (e.g., two crosses, Fig. 3e). Generally then, bilayers can be formed between shaped hydrogel objects in geometries that cannot be achieved with spherical aqueous droplets.

The area and hence the capacitance of a bilayer could be increased or decreased reversibly by pushing together or pulling apart two lipid-coated hydrogel shapes with a micromanipulator (Fig. 3j–l, Supplementary Fig. S2)<sup>18</sup>. A bilayer could be ruptured by pushing the two faces hard against each other. Once ruptured, a bilayer could be quickly reformed by pulling the two hydrogel objects apart and bringing them back together.

**Hydrogel-hydrogel bilayer networks.** Agarose shapes, coated with lipid monolayers ( $10 \text{ mg mL}^{-1}$  DPhPC in hexadecane), were assembled manually (by using a stainless steel needle) to form networks that featured bilayers in series and in branched structures (Fig. 4). Bilayers delimited the individual objects, because no dye transport was observed between them (Fig. 4a,b). Bilayer networks with altered patterns could be constructed by simple manual manipulation of the hydrogel shapes with a needle (Fig. 4c–e). The bilayer networks formed by the millimeter-sized hydrogel shapes were stable for up to 48 h ( $n = 19$ ).

**Hydrogel assemblies without bilayers.** Hydrogel shapes were also used as building blocks to construct self-assembling networks to enable communication over macroscale (centimeter) distances. When agitated or mechanically stirred in hexadecane (with or without lipids), the hydrogel shapes formed arbitrarily arranged networks (Fig. 5a, Supplementary Fig. S3). In this case, no lipid bilayers remained at the hydrogel-hydrogel interfaces after the assembly process. The networks could be altered by manipulation with a steel needle to form assemblies with desired arrangements of the hydrogel objects.

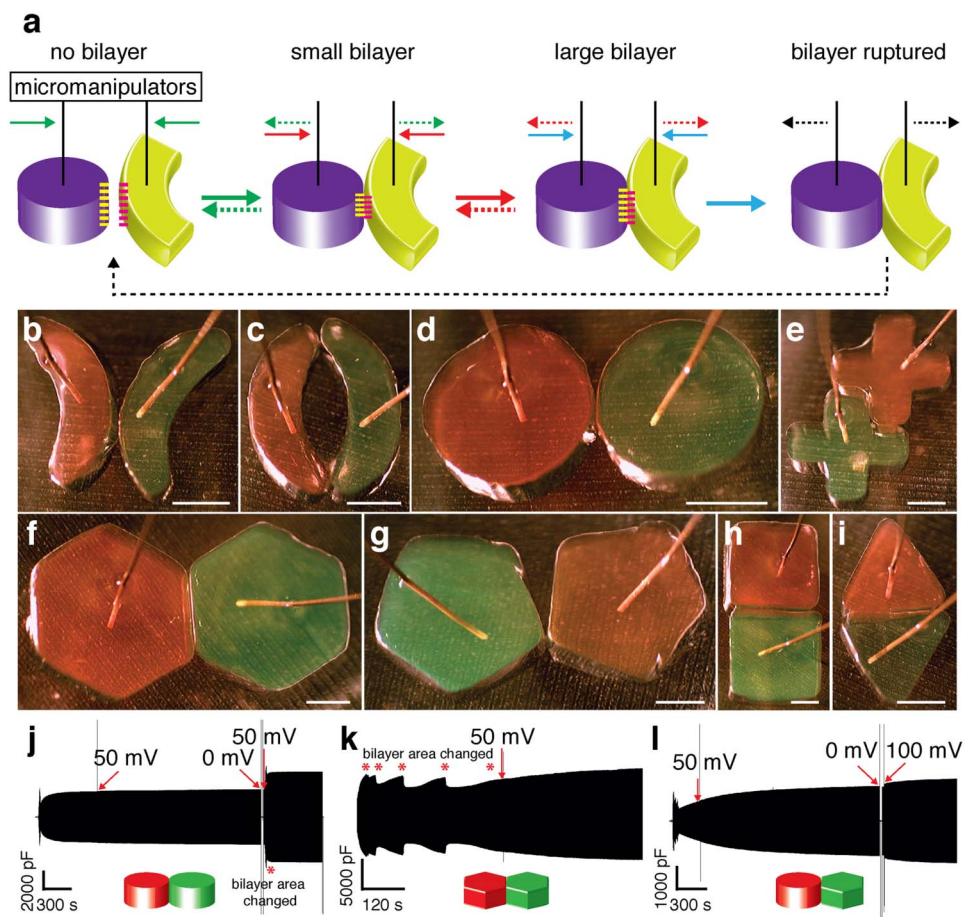


**Figure 3 | Bilayers between hydrogel shapes.** (a) Scheme showing bilayer formation between two hydrogel shapes, and the effect of force on bilayer stability. The bilayer area increased or decreased depending on whether the shapes were pushed against each other or pulled apart. The bold arrows indicate the movement of the agarose shapes connected to Ag/AgCl electrodes, which was caused by adjustments of the micromanipulators in the directions indicated (thin arrows). The colors of the bold and thin arrows correspond. Red and yellow ladders on the shapes denote lipid monolayer leaflets. (b – i) Agarose shapes in a DPhPC/hexadecane mixture ( $5 \text{ mg mL}^{-1}$ ) could be arranged in various configurations to form lipid bilayers of the desired size. (j – l) Hydrogel-hydrogel bilayers were stable up to an applied potential of +150 mV, as monitored by capacitance measurements. The bilayer size was manipulable under an applied transmembrane potential by moving the hydrogel shapes with a micromanipulator. The red asterisks on the capacitance signal (j, k) denote a change in the bilayer area. Scale bars (b – i), 1 mm.

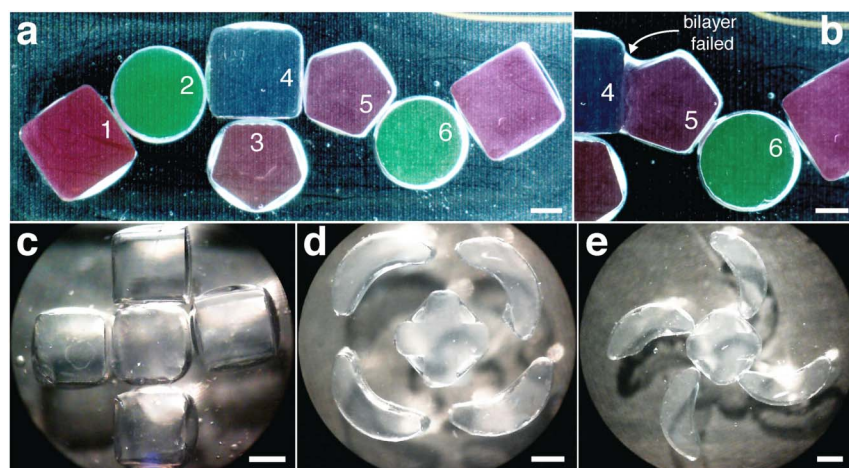


**Figure 4 | Hydrogel-hydrogel bilayer networks.** (a) Agarose shapes (1% w/v) containing fluorescein or 5-carboxytetramethylrhodamine (5% v/v) (5-cTAMRA) were incubated in DPhPC in hexadecane ( $10 \text{ mg mL}^{-1}$ ) and manipulated into chains using a steel needle. The absence of dye transfer across the hydrogel interfaces (labeled 1 – 6) revealed the presence of bilayers. (b) When a bilayer was compromised, dye diffusion from one hydrogel object to the other was discernible in  $\leq 1 \text{ min}$  ( $n = 11$ ). (c) Agarose cubes arranged in a pattern with bilayers at the interfaces. (d) Two different shapes (crescent and cross) were arranged to form a pattern with each crescent forming a bilayer with the cross (e). Scale bars, 1 mm.

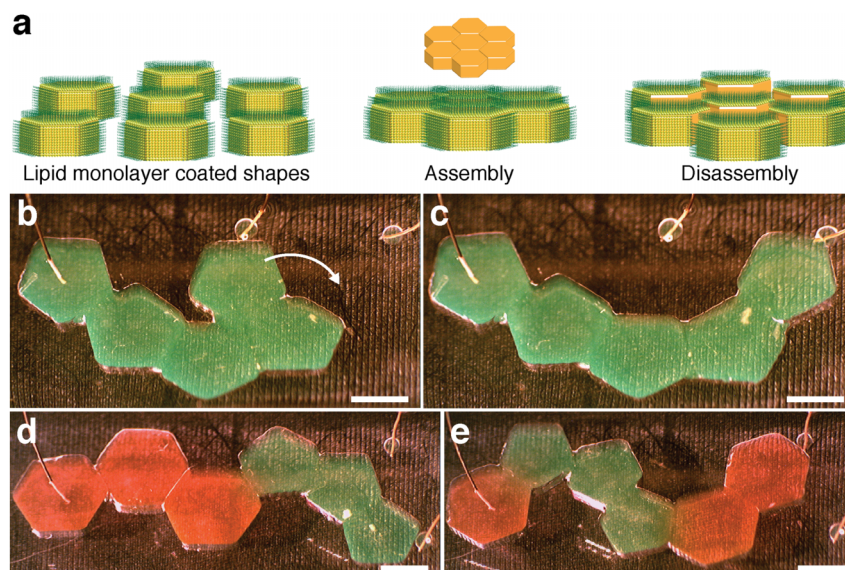


**Figure 5 | Self-assembly of hydrogel shapes.** (a) Lipid-coated hydrogel shapes self-assembled when agitated in hexadecane ( $\leq 5 \text{ mg mL}^{-1}$  DPhPC; at a higher lipid concentration of  $10 \text{ mg mL}^{-1}$  self-assembly was slower owing to a higher viscous drag experienced by the hydrogel objects in the oil). No bilayers were present at the interfaces between hydrogel objects in these self-assembled networks as determined by electrical measurements. (b, c) The assemblies could be rearranged manually with a steel needle (Supplementary Fig. S3), and were by this means used to form switchable electrical networks. As shown here, two agarose spheres (diameter  $700 \mu\text{m}$ ) were formed on a two-armed Ag/AgCl electrode connected to the ground end of the head stage. An assembly of agarose pentagons was penetrated by another Ag/AgCl electrode connected to the active end of the head stage. Sliding a pentagon (white arrow) with a needle changed the network from a compact to an extended configuration, and rewired the network from one grounded sphere to the other. (d, e) The configuration of a hydrogel network, with shapes containing different small molecules (5-cTAMRA and fluorescein), was manipulated with a needle. It was not necessary to remove any of the hydrogel objects from the oil; the shapes slid along each other to reach the final configuration. Scale bars, 2 mm.

Displacement of the lipid bilayer between two hydrogel objects maximizes the area of contact between the hydrophilic surfaces to form a thermodynamically stable configuration<sup>19</sup>.

**Hydrogel electrical circuits.** By utilizing the principles outlined above for hydrogel object assembly with or without lipid bilayers, we were able to construct assemblies in which some hydrogel object pairs were connected by a bilayer whereas others had no bilayers between them (Supplementary Fig. S4). Hydrogel networks without intervening bilayers were assembled in DPhPC ( $5 \text{ mg mL}^{-1}$  in hexadecane). The entire network was thus coated with a lipid monolayer. A stable bilayer between a hydrogel object and such a network was established by carefully controlling the distance between the object and the network with a micromanipulator (Supplementary Fig. S4). The ability to move the hydrogel pieces manually in a network allowed reconfiguration of the electrical connections. For example, a network of pentagons was assembled without bilayers between the objects. An Ag/AgCl electrode was inserted in one of the terminal pentagons, and a bilayer was formed between the other terminal pentagon and one of two agarose spheres (diameter  $\sim 700 \mu\text{m}$ ) on a branched Ag/AgCl electrode (Fig. 5b). By sliding the second pentagon to extend the configuration of the network, a new bilayer between that pentagon and the second agarose sphere was formed, while the first bilayer was broken (Fig. 5c). Similarly, an assembly of hexagons and pentagons was used to demonstrate a different change in configuration (Fig. 5d,e). In addition, an electrical contact was established between a self-assembled network (without bilayers between the shapes) and a hydrogel sphere containing  $\alpha\text{HL}$  pores (Supplementary Fig. S8c,d).

**Hydrogel wire.** Wires are crucial components of any electrical device. Agarose was formed into long wires ( $>1 \text{ cm}$ ) of  $\sim 0.5 \text{ mm}$  diameter by gelling within a capillary and extrusion. The wires were used to connect various hydrogel objects. For example, an

agarose wire could be bent to form bilayers at two points on the same object (Supplementary Fig. S5a,b). An agarose wire could also be used to link two hydrogel assemblies and serve as a flexible hinge to reconfigure the electrical connections (Supplementary Fig. S5c,d). The transmission of information over centimeter distances by agarose wires was shown by the insertion of  $\alpha\text{HL}$  pores into a bilayer formed between an agarose sphere and one end of a wire. Ion flow through the pores was detected by connecting an electrode to the other end of the wire (Supplementary Fig. S8e,f). On a simple level, lipid monolayer-coated agarose wires mimic the axons of neurons (the diameter of a squid giant axon is  $0.5 \text{ mm} - 1 \text{ mm}$ ).

A soft wire is prone to damage. We therefore devised ways to repair a broken wire in a hydrogel circuit. The circuit was constructed by forming a bilayer between an agarose sphere (on an Ag/AgCl electrode) and a hexagon in a two-hexagon assembly (with no bilayer between the objects). An agarose wire was used to connect one of the hexagons to an agarose pentagon penetrated by an Ag/AgCl electrode (Supplementary Fig. S6). The formation of the only bilayer in the system, between the sphere and the hexagon, was monitored by an increase in capacitance. Upon cutting the agarose wire with a blade, and separating the two ends the capacitance fell to the background value. It sufficed to touch the two cut ends together to re-establish the electrical circuit. In a second approach, a broken agarose wire was resealed by connecting the severed ends with a buffer droplet or with a hydrogel object (Supplementary Fig. S6).

Interestingly, we could also reconnect an electrical circuit without apparent contact between the cut agarose wires. A bilayer was formed between a  $\sim 600 \mu\text{m}$ -diameter agarose sphere (on an Ag/AgCl electrode) and a pentagon shape, which was connected to a hexagon (on an Ag/AgCl electrode) via a hydrogel wire (Supplementary Fig. S7a,b). After cutting the wire into two, the severed end of one of the wires was dragged manually to and from the other severed end on the PMMA surface (Supplementary Fig. S7c). This process re-established the electrical connection between the two electrodes

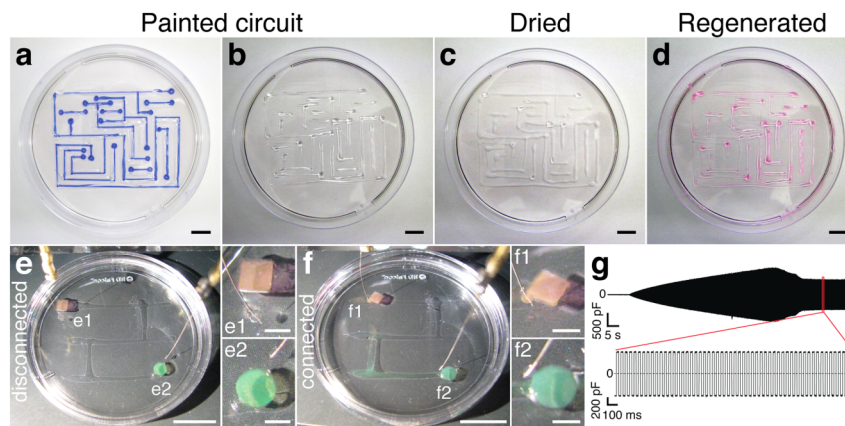


**Figure 6 | Painted circuits.** (a, b) By using a 21-gauge syringe needle, agarose wires (1% w/v) were painted on a circuit diagram (blue) on a Petri plate (the diagram was then removed). (c) The agarose circuit was dried in air, and (d) regenerated by adding buffer (1 M KCl, 10 mM Tris.HCl, pH 7.0, containing 5% v/v 5-cTAMRA). The buffer rehydrated only the dried agarose wires (pink) and did not wet the Petri plate surface. (e) A simple circuit was painted with agarose wires and immersed in hexadecane (1 mg mL<sup>-1</sup> DPhPC). Two hydrogel objects (red cube and green cylinder) were placed at distant points on the circuit. Two agarose spheres (diameter ~800 μm) at the end of Ag/AgCl electrodes were placed in the lipid oil mixture (*insets* e1 and e2). (f) One sphere was pressed hard against the cube such that no bilayer remained between the two objects (*inset* f1, the diffusion of dye into the sphere indicates that no bilayer was present), while a bilayer was formed between the second agarose sphere and the cylinder (*inset* f2, no color change of this sphere demonstrates the formation of a lipid bilayer barrier). Bilayer formation was further confirmed by a specific capacitance measurement of 0.65 μF cm<sup>-2</sup> (g). The diffusion of dye from the hydrogel cube and cylinder into the wires was observed after a few minutes indicating that there were no bilayers at these junctions. Scale bars (a – f), 1 cm; (e1, e2, f1, f2), 2 mm.

indicated by a specific capacitance of ~0.4 μF cm<sup>-2</sup> for the lipid bilayer between the agarose sphere and the pentagon (Supplementary Fig. S7g). A similar phenomenon was observed after dragging an agarose object connected to an agarose wire. For example, a bilayer was formed between an agarose sphere (on an Ag/AgCl electrode) and a pentagon, which was connected to another pentagon (on an Ag/AgCl electrode) by an agarose wire (Supplementary Fig. 7a,d). The pentagon on the electrode was dragged to and from the end of the agarose wire by using a micromanipulator. After this procedure, a specific capacitance value of ~0.7 μF cm<sup>-2</sup> diagnostic of a bilayer was recorded even though the pentagon was not touching the agarose wire (Supplementary Fig. 7d,h). Dragging a piece of agarose on a PMMA surface, most probably painted thin, lipid-stabilized aqueous tubes along the surface thereby forming conductive paths between the two electrodes. We tested this idea by removing the electrode from the hydrogel pentagon and touching it on the PMMA surface where the hydrogel had been dragged. No change in the bilayer capacitance was observed signifying the presence of an electrical connection. After touching the electrode to a part of the PMMA surface where the hydrogel had not been dragged, the capacitance decreased to the basal value (Supplementary Fig. S7a,e,f,i).

**Painted circuits.** Inspired by this finding, we made hydrogel-painted circuits (2 cm × 2 cm to 6 cm × 5 cm) analogous to conventional printed circuits boards (Fig. 6). Agarose wires (diameter ~1–2 mm) were painted on a Petri plate with a 21-gauge needle (Fig. 6a,b). Interestingly, when the agarose wires were dried, they could be regenerated as conducting material by adding buffer or water to the dish (Fig. 6c,d). Small molecules (e.g., fluorescein or 5-cTAMRA) could be incorporated uniformly into the wires by inclusion in the original agarose or in the regenerating buffer. A proof-of-concept circuit was made by painting agarose wires onto a Petri plate, and placing two agarose shapes (a cube with 5-cTAMRA and a cylinder with fluorescein) at either end of the circuit. A bilayer was formed between an agarose sphere (on an Ag/AgCl electrode) and the cylinder (green) (Fig. 6e,f). To establish the integrity of the bilayer, a second agarose sphere (on an Ag/AgCl electrode) was connected to the cube (with no bilayer in this case). A capacitance of ~0.7 μF cm<sup>-2</sup> confirmed both a bilayer formation at the cylinder

and an electrical connection between the cylinder and the cube through the agarose wires (Fig. 6g). Such lipid-coated hydrogel wires connected to each other may be used to mimic neural circuits.

**Mechanical devices.** The frameworks of conventional machines and their parts (gears, screws, nuts, bolts, etc.) are made of hard components. We show here that soft components, hydrogel objects, can be used as mechanical components to switch electrical circuits. For example, a cross-shaped hydrogel object, covered with a lipid monolayer, was used as a manual switch in an electrical circuit (Fig. 7a,b). Such a switch was able to form two bilayers simultaneously with two agarose spheres (Fig. 7c). Further, a magnetically-actuated switch was made by assembling a rectangular hydrogel bar and a hydrogel cube loaded with paramagnetic beads. There was no bilayer between the two hydrogel objects (Fig. 7d). The magnetic gel cube served as an actuator by causing the whole assembly to move under a magnetic field. The empty rectangular hydrogel bar connected, electrically and reversibly, two agarose spheres by the formation of lipid bilayers (Fig. 7e–g, Supplementary Movie 1). A cross-shaped switch was made in a similar manner but with two magnetic actuator cubes (Fig. S9, Supplementary Movie 2). Simple mechanical elements such as these might be incorporated into the electrical circuits of functional devices.

A rotating device was constructed from a hydrogel cross and four crescents (Supplementary Fig. S10). In this case, no bilayers were present between the cross and the crescent shapes of the rotor (cf. Fig. 4e). A crucial difference between the two assemblies formed of a cross and crescents (Fig. 4 and Supplementary Fig. S10) is the contact area between their constituent shapes. The contact area was smaller in the bilayer network (Fig. 4e), which prevented expulsion of the bilayers and adhesion owing to surface tension, a dominant force when the hydrogel pieces have a large surface area<sup>20</sup>. Automated rotation of the rotor was achieved by using a magnetic field. The objects forming the rotor were loaded with paramagnetic beads and the structure was rotated with a neodymium (Nd) magnet attached to a motor. When the magnet's axis was tilted at an angle ( $\theta \sim 30^\circ$ ) to the structure's axis of rotation, the hydrogel rotor rotated, whereas at  $\theta = 0$ , the rotor did not rotate (Fig. 8a). The direction of rotation of the structure, clockwise or counter-clockwise, depended on the

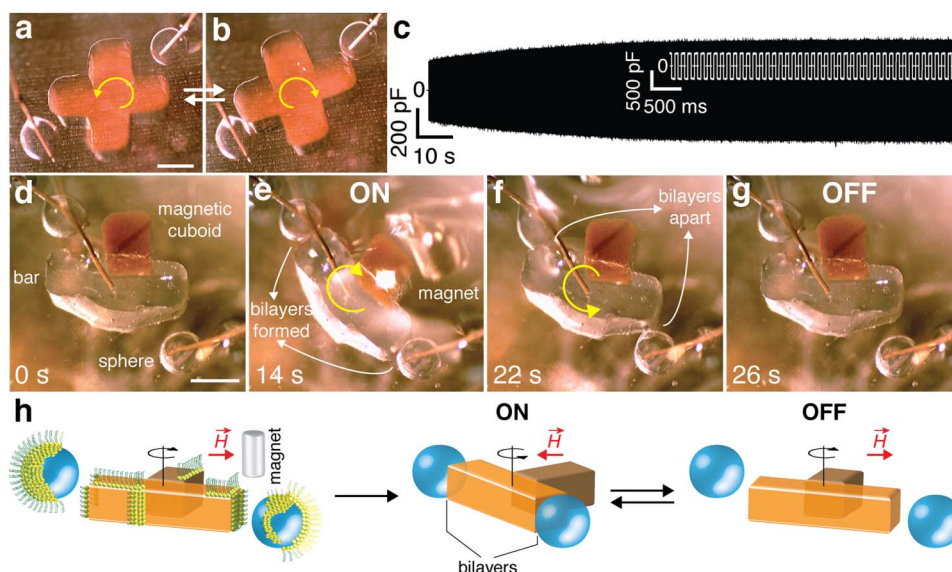


**Figure 7 | Soft-matter mechanical devices.** (a, b) An agarose cross (colored with 5-cTAMRA) was used as a switch to connect and disconnect two agarose spheres (diameter  $\sim 1$  mm) on Ag/AgCl electrodes; one sphere was connected to the ground and the other to the active end of a head stage. An electrical circuit was formed when the two poles of the cross formed bilayers with the spheres ( $1 \text{ mg mL}^{-1}$  DPhPC in hexadecane). In this case, the rotation of the hydrogel switch was performed manually using a steel needle. (c) Representative trace showing an increase in electrical capacitance during bilayer formation. The white overlay shows a magnified region of the capacitance signal signifying a tight seal of the bilayer. We automated the ‘ON-OFF’ function of the hydrogel switch by using a magnetic field. (d) The switch was made by connecting a hydrogel cube loaded with paramagnetic beads and an empty hydrogel bar. The placement of the magnetic beads in only one hydrogel piece increased the spatial resolution with which the switch could be controlled. The switch was immersed in a lipid/oil mixture ( $1 \text{ mg mL}^{-1}$  DPhPC in 1 : 1 v/v hexadecane/silicone oil AR20). A Ag/AgCl wire (not connected to the headstage) was inserted in the empty hydrogel bar to act as an axle. (e) A cylindrical Nd magnet (height 5 mm, radius 2.5 mm) was used to rotate the switch clockwise so that the poles of the hydrogel bar formed bilayers (‘ON’ state) with the hydrogel spheres. (f, g) A counter-clockwise rotation of the switch separated the leaflets disconnecting the circuit (‘OFF’ state). Yellow arcs with arrowheads denote the clockwise and counter-clockwise rotation of the switch. The time in seconds is shown. The ‘ON-OFF’ cycle was repeated several times (Supplementary Movie 1). (h) Representation of the reversible bilayer formation using the switch. Scale bars (a and d), 1 mm.

angular velocity of the Nd magnet. When the magnet was rotated slowly in the clockwise direction, the structure rotated anti-clockwise (Fig. 8b–f). On increasing the clockwise angular velocity of the magnet, the rotation switched to the clockwise direction (Fig. 8g–k, Supplementary Movie 3). Such a magnetic rotor could be used to form bilayers sequentially between its blades and a hydrogel sphere (Fig. 8l–p).

The magnetic hydrogel rotor was used to perform work as a droplet-collecting unit. The lipid monolayer-coated hydrogel crescents of the rotor were used as sticky fingers to pick up lipid-encased aqueous droplets. Aqueous droplets strewn around the rotor were collected in the cusps of the structure as a result of the centripetal force generated during rotation under a magnetic field (Supplementary Fig. S11, Supplementary Movie 4). The collection process was facilitated by the formation of bilayers between the hydrogel shape and the droplets. If a droplet was too far away to experience the centripetal force of the rotating device, the magnet was stopped at the droplet location. This slowly dragged the hydrogel rotor towards the magnet, and the droplet then attached to the rotor by forming a bilayer with the crescent. The rotation of the magnet was re-started to capture the droplet (Supplementary Fig. S12). These experiments demonstrate the feasibility of using soft-matter components to fabricate mechanical devices for use in bottom-up assembly of bilayer networks.

## Discussion

In bottom-up synthetic biology, attempts are being made to use biological parts or materials to build materials ranging from nano-devices to minimal cells and tissues<sup>4,21,22</sup>. Our interest is in synthetic minimal tissues. Droplet networks are a favorable framework for exploration of the potential of such entities<sup>8</sup>. Non-hydrogel droplet networks have been produced that store and use energy<sup>8</sup>, that form

simple electrical circuits<sup>15</sup>, and that respond to signals such as light<sup>8</sup> or deliver chemicals to an external aqueous medium<sup>16</sup>. In previous work, bilayers were formed from lipid monolayers assembled on a hydrogel surface and individual aqueous droplets for single-molecule electrical and fluorescence experiments<sup>14</sup>.

In the present work, we have constructed bilayer networks by using shaped hydrogel objects as building blocks, rather than fluid aqueous droplets. Hydrogels have been used in numerous biomedical applications including drug delivery<sup>23,24</sup> and the provision of scaffolds for tissue engineering<sup>25,26</sup>. The assembly of shaped objects by the minimization of interfacial free energy was pioneered by Whitesides and colleagues<sup>27,28</sup>. Based on these studies, Khademhosseini made microgel pieces from a poly(ethylene glycol)-methacrylate polymer and had them self-assemble in mineral oil<sup>19</sup>. The assemblies were unstable when transferred to water, unless first crosslinked at the interfaces. These assemblies may prove useful for scaffolding living cells in tissue-like 3D patterns *in vitro*<sup>19</sup>. To our knowledge, the examples in the present report demonstrate for the first time the use of hydrogels in forming electrical and mechanical units. In conjunction with lipids and proteins such units can form the basis of more elaborate electrical circuits and soft-matter mechanical devices.

With respect to synthetic minimal tissues, hydrogel shapes are robust biocompatible building blocks with forms that cannot be retained by purely aqueous droplets. The hydrogel endows an aqueous compartment with a primitive cytoskeleton. Here, we have shown that hydrogel shapes can be assembled into structures in which the building blocks can be separated with lipid bilayers. The structures can be readily rearranged and communication through the interface bilayers can be achieved with protein pores, as realized previously with aqueous droplets. By this means, electrical signaling through the structures or to contacting electrodes is possible. The

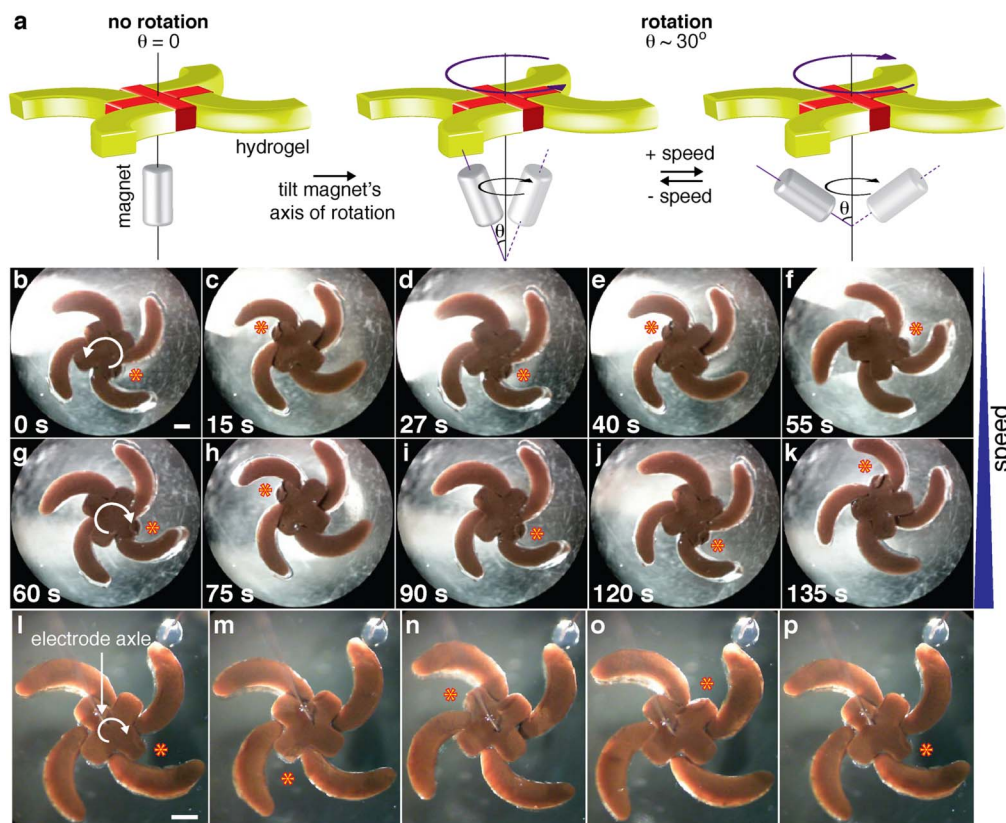


**Figure 8 | Reversible rotation of a hydrogel rotor.** (a) A hydrogel cross and four crescents were used to construct a rotor. The rotor, loaded with paramagnetic beads, moved under an external magnetic field. The rotation depended on the magnet's axis of rotation: when  $\theta = 0$ , the assembly did not rotate; when  $\theta \sim 30^\circ$ , the assembly rotated. The direction of rotation of the hydrogel assembly changed with the magnet's angular velocity. At lower speeds the assembly rotated counter to the rotation of the magnet (clockwise), but at higher speeds the assembly switched its direction of rotation to match that of the magnet. (b–k) Movie snapshots (Supplementary Movie 3) of the rotor's counter clockwise and clockwise rotation at slow and fast speeds of the magnet, respectively. The time in seconds is shown. (l–p) Four crescents and a cross (both shapes contained magnetic beads) were assembled manually to form a rotor, which was rotated manually around an Ag/AgCl axle, which also acted as an electrode. The mechanical assembly was coated with a lipid monolayer in a lipid/hexadecane mixture ( $1 \text{ mg mL}^{-1}$  DPhPC). The blades of the rotor connected sequentially with a sphere (also lipid-coated) on an Ag/AgCl electrode as shown by the formation of a bilayer with specific capacitance  $\sim 0.6 \mu\text{F cm}^{-2}$ . The colored star denotes a defect in the cross shape used as a reference point to follow the rotation. Scale bars (b and l), 1 mm.

versatility of the signaling was enhanced by the use of extruded hydrogel wires or painted hydrogel connections. These wires and connections are analogs of neurons. The objects could also be made into mechanical devices, such as a rotor with alternating electrical contacts, which again could not be achieved without the rigidity of the hydrogel interior.

The work initiated in this paper might be extended in several directions. The assembly of hydrogel objects might be controlled by shape<sup>29</sup>, surface energy<sup>30,31</sup> or molecular recognition<sup>32,33</sup>. Temperature, pH, light, chemicals, ions, and magnetic or electrical fields have been shown to act as stimuli for switching the shapes of hydrogels and might therefore be used to control assembly<sup>34–37</sup>, as might surfaces with switchable properties<sup>38,39</sup>. One long-term goal is the fabrication of biocompatible synthetic tissues for the delivery of therapeutic agents. Such synthetic tissues would have to be adapted to work in an aqueous environment, which has already been achieved with droplet networks<sup>16</sup>. The synthetic tissues might be autonomous or operate through external impetuses, such as light<sup>8</sup> or a magnetic field (as shown here). Alternatively, synthetic tissues might be connected to electronic interfaces<sup>15</sup>. Again, a direct interface between natural and synthetic tissues might be made, in which case the shape of the hydrogel compartments in contact with natural cells would be all important<sup>35</sup>. The ability to change shape, by further analogy with the cytoskeleton, might also be useful in this regard.

## Methods

**Molding hydrogel shapes.** Millimeter-sized hydrogel shapes were fabricated with low melt agarose (1% w/v unless stated otherwise) (Sigma, Dorset, UK) in poly(methyl methacrylate) (PMMA) molds. A CNC machine was used to manufacture PMMA molds with the desired shapes (Supplementary Fig. S1). The agarose (dissolved in 1 M KCl, 10 mM Tris.HCl, pH 7.0) was melted and poured into the mold. After gelling, the shapes were removed and immediately immersed in hexadecane ( $\geq 99\%$ ) (Sigma-Aldrich, Dorset, UK), with or without dissolved lipids. The agarose wires were made in 0.5 mm (I.D.) borosilicate capillary tubes. Warm agarose solution was drawn into a tube by capillary action and allowed to gel. The capillary was broken, and the gelled wire pushed out by using a syringe needle.

**Lipid bilayers between two hydrogel surfaces and electrical recording.** The agarose shapes were incubated in a lipid/hexadecane mixture ( $1$  to  $10 \text{ mg mL}^{-1}$  DPhPC, Avanti Polar Lipids, Alabama, USA) for  $>1$  h. To monitor bilayer formation, after incubation, two hydrogel shapes were impaled with Ag/AgCl electrodes and slowly brought into contact by using a micromanipulator. Bilayer formation was detected by an increase in the specific capacitance to a value of  $\sim 0.6 \mu\text{F cm}^{-2}$ . To record currents passed by  $\alpha\text{HL}$  pores, wild-type or a mutant (2N) heptameric  $\alpha\text{HL}$  protein ( $\sim 200 \text{ nL}$ ) in liposomes made with DPhPC ( $1 \text{ mg mL}^{-1}$ ), was absorbed on an agarose sphere (diameter 0.6–1.5 mm) and incubated in the lipid/hexadecane mixture for 10 to 15 min. Upon touching the agarose sphere to a lipid-monolayer-coated agarose object,  $\alpha\text{HL}$  insertion was observed by current recording. The current was amplified by using a patch-clamp amplifier (Axopatch 200B, Axon Instruments, USA), filtered with a low-pass Bessel filter (80 dB/decade) with a corner frequency of 1 kHz, and digitized with a Digidata 1322 A/D converter (Axon Instruments) at a sampling frequency of 10–20 kHz. In some cases, the data were low-pass filtered post-acquisition at 50 Hz.

**Preparation of  $\alpha\text{HL}$  proteins.** The WT- $\alpha\text{HL}$  heptamer was produced by purifying spontaneously oligomerized  $\alpha\text{HL}$  from *Staphylococcus aureus* Wood 46 cultures as





described elsewhere<sup>40</sup>. After purification the heptamer was stored in 20 mM sodium phosphate buffer, 150 mM NaCl, 0.3% (w/v) SDS, pH 8.0 at  $-80^{\circ}\text{C}$ . The E111N/K147N (2N)  $\alpha$ HL mutant was expressed as monomers in an *Escherichia coli* in vitro transcription translation system (IVTT) and assembled into heptamers on rabbit red blood cell membranes<sup>41</sup>.

- Whitesides, G. M. & Grzybowski, B. Self-assembly at all scales. *Science* **295**, 2418–2421 (2002).
- Alberts, B. *et al. Molecular biology of the cell*, Edn. 3. (Garland Publishing Inc., New York, London; 1994).
- Schwille, P. Bottom-up synthetic biology: engineering in a tinkerer's world. *Science* **333**, 1252–1254 (2011).
- Woolfson, D. N. & Bromley, E. H. C. Synthetic biology: a bit of rebranding, or something new and inspiring? *The Biochemist* **33**, 19–25 (2011).
- Chiarabelli, C., Stano, P. & Luisi, P. L. Chemical approaches to synthetic biology. *Curr Opin Biotechnol* **20**, 492–497 (2009).
- Noireaux, V., Maeda, Y. T. & Libchaber, A. Development of an artificial cell, from self-organization to computation and self-reproduction. *Proc Natl Acad Sci USA* **108**, 3473–3480 (2011).
- Zostak, J. W., Bartel, D. P. & Luisi, P. L. Synthesizing life. *Nature* **409**, 387–390 (2001).
- Holden, M. A., Needham, D. & Bayley, H. Functional bionetworks from nanoliter water droplets. *J Am Chem Soc* **129**, 8650–8655 (2007).
- Leptihn, S., Thompson, J. R., Ellory, J. C., Tucker, S. J. & Wallace, M. I. In vitro reconstitution of eukaryotic ion channels using droplet interface bilayers. *J Am Chem Soc* **133**, 9370–9375 (2011).
- Harriss, L. M., Cronin, B., Thompson, J. R. & Wallace, M. I. Imaging Multiple Conductance States in an Alamethicin Pore. *J Am Chem Soc* **133**, 14507–14509 (2011).
- Heron, A. J., Thompson, J. R., Mason, A. E. & Wallace, M. I. Direct detection of membrane channels from gels using water-in-oil droplet bilayers. *J Am Chem Soc* **129**, 16042–16047 (2007).
- Bayley, H. *et al.* Droplet interface bilayers. *Mol BioSystems* **4**, 1191–1208 (2008).
- Syeda, R., Holden, M. A., Hwang, W. L. & Bayley, H. Rapid screening of blockers against a potassium channel with a droplet interface bilayer array. *J Am Chem Soc* **130**, 15543–15548 (2008).
- Heron, A. J., Thompson, J. R., Cronin, B., Bayley, H. & Wallace, M. I. Simultaneous measurement of ionic current and fluorescence from single protein pores. *J Am Chem Soc* **131**, 1652–1653 (2009).
- Maglia, G. *et al.* Droplet networks with incorporated protein diodes show collective properties. *Nat Nanotechnol* **4**, 437–440 (2009).
- Villar, G., Heron, A. & Bayley, H. Formation of droplet networks that function in aqueous environments. *Nat Nanotechnol* **6**, 803–808 (2011).
- Thompson, J. R., Heron, A. J., Santos, Y. & Wallace, M. I. Enhanced stability and fluidity in droplet on hydrogel bilayers for measuring membrane protein diffusion. *Nano Lett* **7**, 3875–3878 (2007).
- Gross, L. C., Heron, A. J., Baca, S. C. & Wallace, M. I. Determining membrane capacitance by dynamic control of droplet interface bilayer area. *Langmuir* **27**, 14335–14342 (2011).
- Du, Y., Lo, E., Ali, S. & Khademhosseini, A. Directed assembly of cell-laden microgels for fabrication of 3D tissue constructs. *Proc Natl Acad Sci USA* **105**, 9522–9527 (2008).
- Bowden, N., Terfort, A., Carbeck, J. & Whitesides, G. M. Self-assembly of mesoscale objects into ordered two-dimensional arrays. *Science* **276**, 233–235 (1997).
- Payne, G. F. Biopolymer-based materials: the nanoscale components and their hierarchical assembly. *Curr Opin Chem Biol* **11**, 214–219 (2007).
- Wu, L.-Q. & Payne, G. F. Biofabrication: using biological materials and biocatalysts to construct nanostructured assemblies. *Trends Biotechnol* **22**, 593–599 (2004).
- Tokarev, I. & Minko, S. Stimuli-responsive porous hydrogels at interfaces for molecular filtration, separation, controlled release, and gating in capsules and membranes. *Adv Mater* **22**, 3446–3462 (2010).
- Zelikin, A. N., Price, A. D. & Städler, B. Poly(methacrylic acid) polymer hydrogel capsules: drug carriers, sub-compartmentalized microreactors, artificial organelles. *Small* **6**, 2201–2207 (2010).
- Wheeldon, I., Farhadi, A., Bick, A. G., Jabbari, E. & Khademhosseini, A. Nanoscale tissue engineering: spatial control over cell-materials interactions. *Nanotechnology* **22**, 212001 (2011).
- Zhu, J. & Marchant, R. E. Design properties of hydrogel tissue-engineering scaffolds. *Expert Rev Med Devices* **8**, 607–626 (2011).
- Choi, I. S., Bowden, N. & Whitesides, G. M. Macroscopic, hierarchical, two-dimensional self-assembly. *Angew Chem Int Ed* **38**, 3078–3081 (1999).
- Bowden, N., Weck, M., Choi, I. S. & Whitesides, G. M. Molecule-mimetic chemistry and mesoscale self-assembly. *Acc Chem Res* **34**, 231–238 (2001).
- Sacanna, S., Irvine, W. T., Chaikin, P. M. & Pine, D. J. Lock and key colloids. *Nature* **464**, 575–578 (2010).
- Tuteja, A., Choi, W., Mabry, J. M., McKinley, G. H. & Cohen, R. E. Robust omniphobic surfaces. *Proc Natl Acad Sci USA* **105**, 18200–18205 (2008).
- Williamson, A. J., Wilber, A. W., Doye, J. P. K. & Louis, A. A. Templated self-assembly of patchy particles. *Soft Matter* **7**, 3423–3431 (2011).
- Leunissen, M. E. *et al.* Switchable self-protected attractions in DNA-functionalized colloids. *Nat Mater* **8**, 590–595 (2009).
- Harada, A., Kobayashi, R., Takashima, Y., Hashidzume, A. & Yamaguchi, H. Macroscopic self-assembly through molecular recognition. *Nat Chem* **3**, 34–37 (2011).
- Sidorenko, A., Krupenkin, T., Taylor, A., Fratzl, P. & Aizenberg, J. Reversible switching of hydrogel-actuated nanostructures into complex micropatterns. *Science* **315**, 487–490 (2007).
- Yoo, J.-W. & Mitragotri, S. Polymer particles that switch shape in response to a stimulus. *Proc Natl Acad Sci USA* **107**, 11205–11210 (2010).
- Jeong, B. & Gutowska, A. Lessons from nature: stimuli-responsive polymers and their biomedical applications. *Trends Biotechnol* **20**, 305–311 (2002).
- Russev, M.-M. & Hecht, S. Photoswitches: from molecules to materials. *Adv Mater* **22**, 3348–3360 (2010).
- Lahann, J. *et al.* A reversible switching surface. *Science* **299**, 371–374 (2003).
- Szynyska, A., Stamm, M., Diez, S. & Ionov, L. Simple and fast method for the fabrication of switchable bicomponent micropatterned polymer surfaces. *Langmuir* **23**, 5205–5209 (2007).
- Maglia, M. *et al.* DNA strands from denatured duplexes are translocated through engineered protein nanopores at alkaline pH. *Nano Lett* **9**, 3831–3836 (2009).
- Stoddart, D., Heron, A., Mikhailova, E., Maglia, G. & Bayley, H. Single nucleotide discrimination in immobilized DNA oligonucleotides with a biological nanopore. *Proc Natl Acad Sci USA* **106**, 7702–7707 (2009).
- Gu, L.-Q., Braha, O., Conlan, S., Cheley, S. & Bayley, H. Stochastic sensing of organic analytes by a pore-forming protein containing a molecular adapter. *Nature* **398**, 686–690 (1999).

## Acknowledgements

H.B. acknowledges support from the European Commission's FP7 READNA Consortium. K.T.S. was supported by a Long-Term FEBS fellowship and a Marie Curie Intra-European Fellowship.

## Author contributions

H.B. and K.T.S. devised the original idea. K.T.S. developed the ideas, designed and performed the experiments, and analyzed the data. K.T.S. and H.B. wrote the paper.

## Additional information

**Supplementary information** accompanies this paper at <http://www.nature.com/scientificreports>

**Competing financial interests:** The authors declare no competing financial interests.

**License:** This work is licensed under a Creative Commons Attribution-NonCommercial-NoDerivative Works 3.0 Unported License. To view a copy of this license, visit <http://creativecommons.org/licenses/by-nc-nd/3.0/>

**How to cite this article:** Sapra, K.T. & Bayley, H. Lipid-coated hydrogel shapes as components of electrical circuits and mechanical devices. *Sci. Rep.* **2**, 848; DOI:10.1038/srep00848 (2012).